Use of Integrated Approaches for Investigating the Role of Conformational Flexibility in Metal Binding and Release Mechanisms in Proteins

Zehra Sayers
Sabanci University, Istanbul, Türkiye
zehra@sabanciuniv.edu

Outline

Function and scales in biological systems.

Structure-function relationships.

Tools for bridging different “structure” and “time” scales in bio-molecular functions.

Results on 2 challenging examples: metallothioneins and ferric binding proteins.

Conclusions.

Functional Elements & Scales in Biological Systems

Static

Integrity and Stability
Cytoskeleton
Connective tissue
Bone/tendon
L: nm-m, T: min-infinite

Dynamic

Molecular Machines (Long range)
Cell division
Transport
Cell Movement
L: nm-m, T: sec-min

Molecular Machines (Short range)
Molecular switches
Signaling
Ion pumps
Catalysis
Polymerization
L: nm-μm, T: nsec-msec

Need for tools (experimental and theoretical) providing data at **different length and time scales.**

https://arcella.nl/amoeba-proteus/

Goal: Understanding and Predicting Function

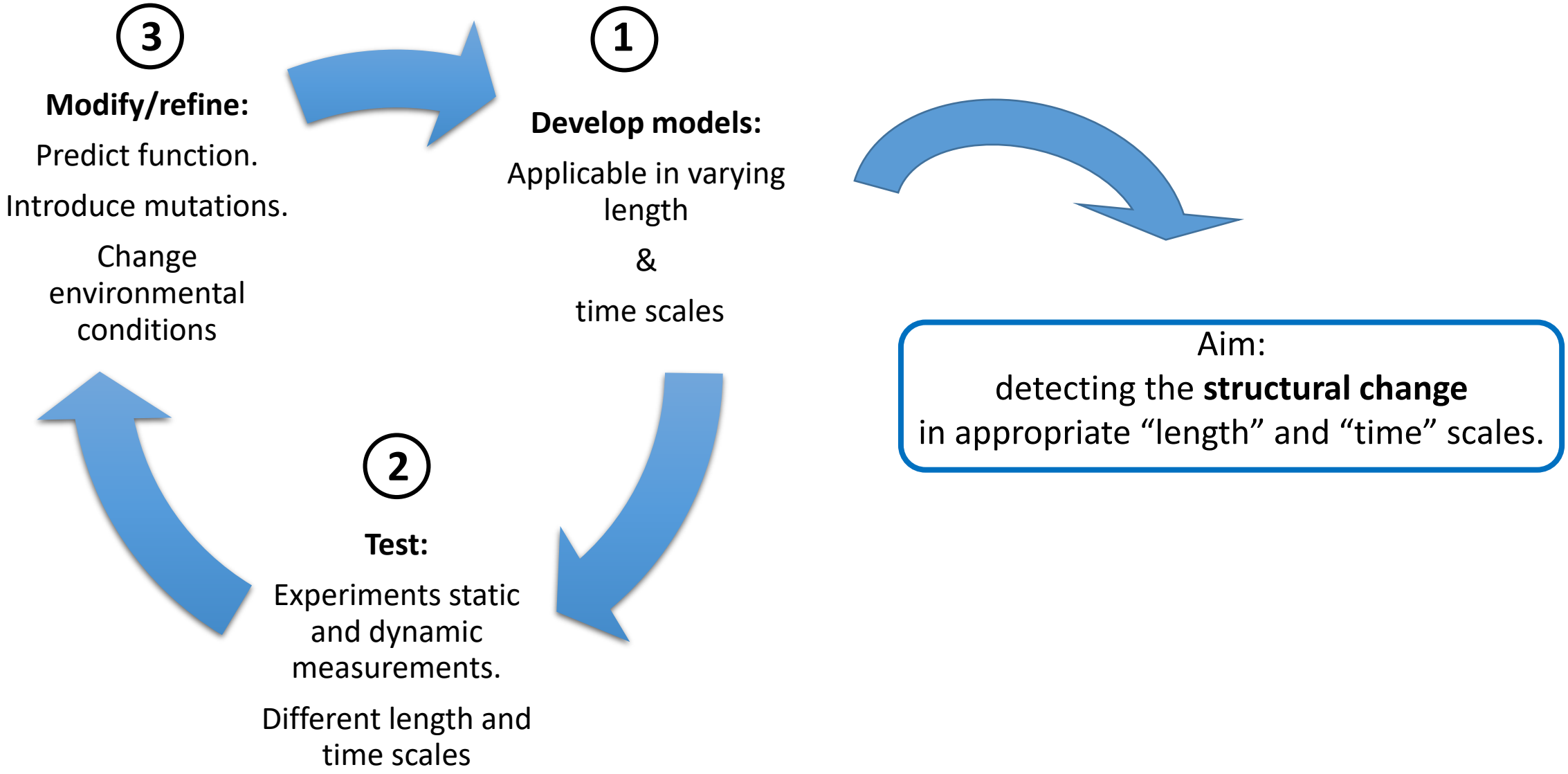

Aim:
detecting the **structural change**
in appropriate “length” and “time” scales.

Tools for Different Length Scales

S.J. Ziegler, S. J.B. Mallinson, P.C. St. John et al. Computational and Structural Biotechnology Journal 19 (2021) 214–225

MX*

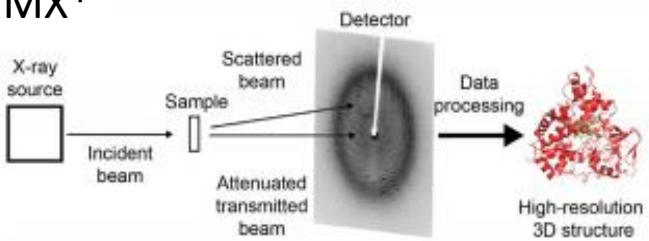

SAXS-SANS*

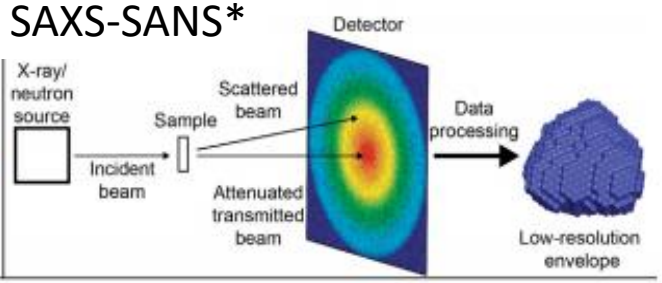

NMR

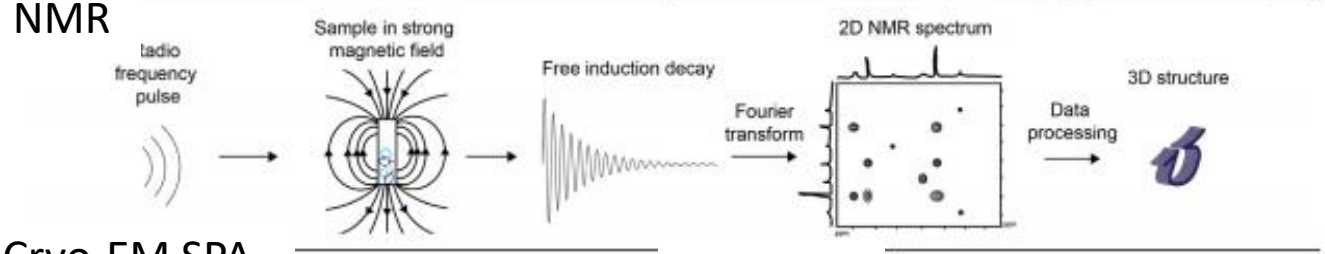

Cryo-EM SPA

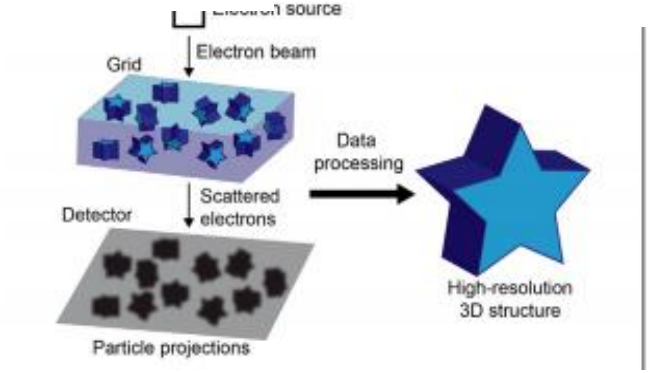

Modeling

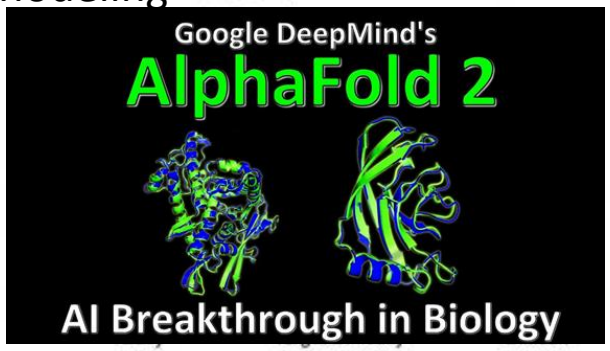

Cryo-EM & tomography

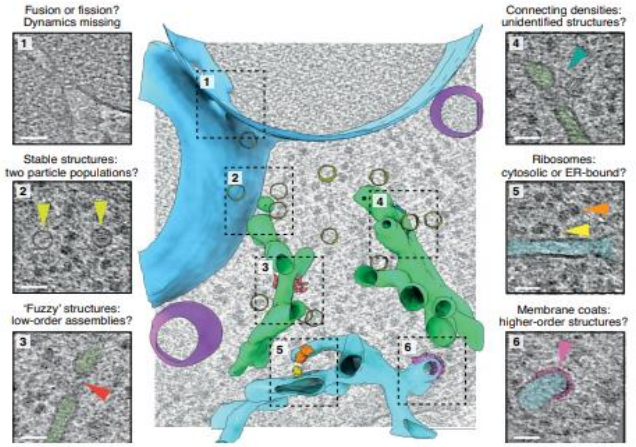

Wozny, M.R. &Kukulski, W. (2021) Nat. Meh. 18:430-31

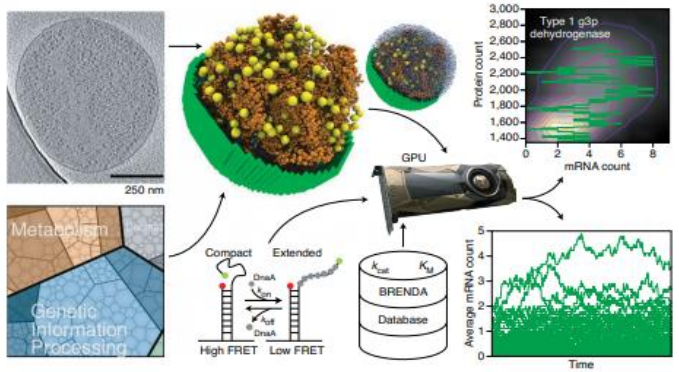

Luthey-Schulten, Z (2021) Nat. Meh. 18:431-443

Closing the length scale gap between molecular structure and cell and tissue architecture.

*SR tools

Tools for Different Time Scales

Time-resolved structural experiments:
Macromolecular Crystallography (MX)*,
Small angle X-ray scattering (SAXS)*,
Cryo-electron microscopy (Cryo-EM),
Nuclear Magnetic Resonance (NMR).
Stopped-flow/pump probe*, XFEL…

Time scales: femtosec-hrs

Molecular Dynamics simulations

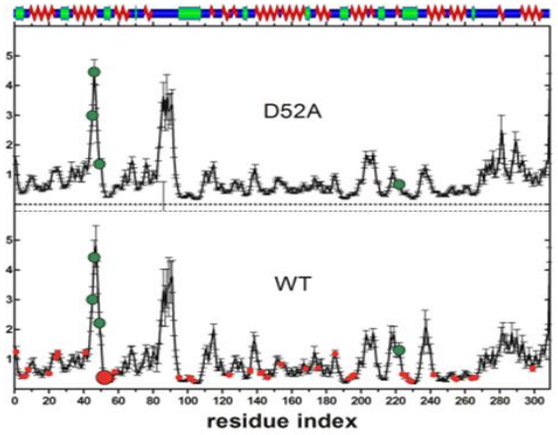

Local conformational flexibility
Simulations for structural dynamics

Güven et al., 2014

Key word: Structural change
Integrated studies aim at closing the gap between **static description** and **functional dynamics** in biological systems.

*SR tools

Structure-Function Relationships in Metal Binding Proteins

Small angle synchrotron X-ray scattering complemented with different biophysical/biochemical techniques and model calculations.

Metallothioneins from wheat → Cd-binding small molecular weight intrinsically disordered proteins lacking secondary structure elements. Difficult to handle. Not suitable for structure analyses by crystallography.

Ferric binding protein (FbpA) from *H. influenzae* → Fe-transport proteins. Crystal structures available but lacking data on conformational flexibility the presence of multiple conformations in solution. Collaboration with C. Atılgan @Sabanci University.

Triticum durum (pasta wheat) Metallothionein (dMT)

Metallothioneins (MTs) are small (6-8 kD) ubiquitous proteins for metal binding (bacteria, yeast and higher organisms, plants).
Metal-sulfur clusters are formed through Cys-X-Cys motifs.

Question: Do MTs participate in Cd resistance in wheat? What does the structure of dMT reveal about its Cd binding and release mechanisms?

T. durum type I metallothionein (dMT) has two metal binding regions (Cys-motifs) connected with a 42 aa long hinge region with one Phe and no Cys.

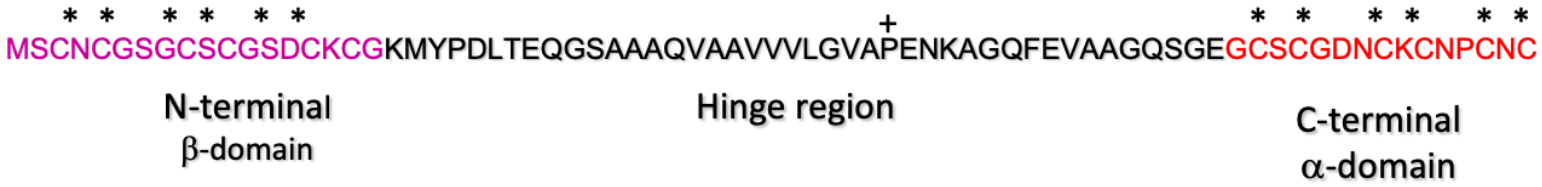

dMT has no secondary structure elements in apo or holo forms.

Yeşilırmak, F. (2008)
Aydın, M. (2011)

Identification and expression of *dMT*

Identification of the *mt* gene in T. durum genome

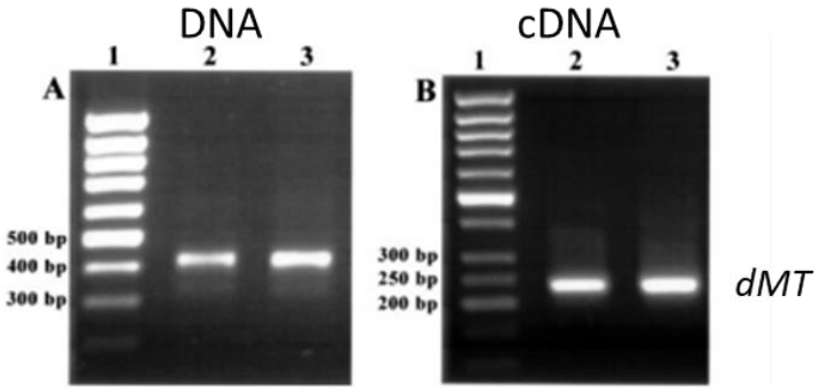

Bacteria synthesizing recombinant dMT survive in medium containing high levels of Cd.

T. durum cv. Balcali85 wheat growth under Cd application.

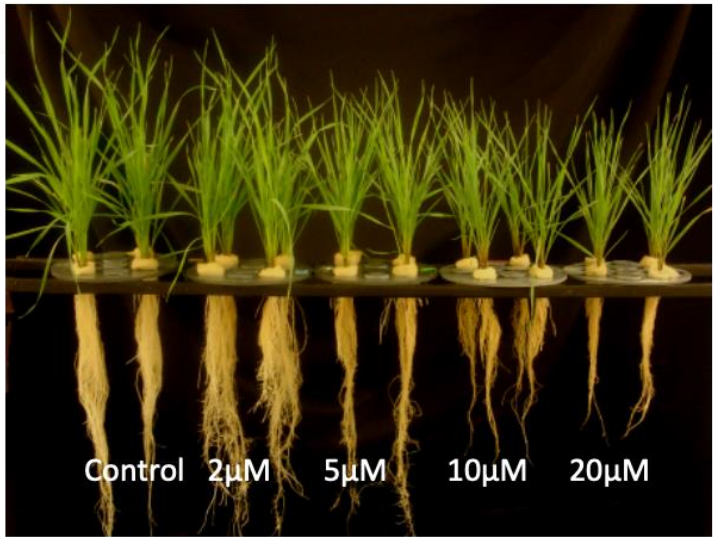

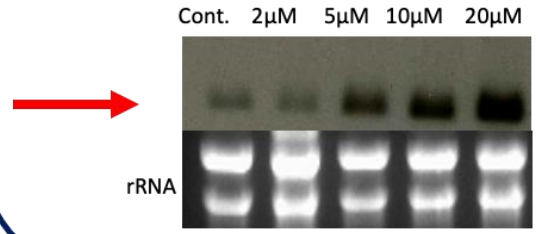

Expression of *dmt* is correlated with accumulation of Cd^{2+} in

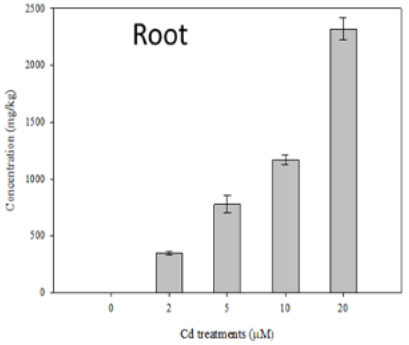

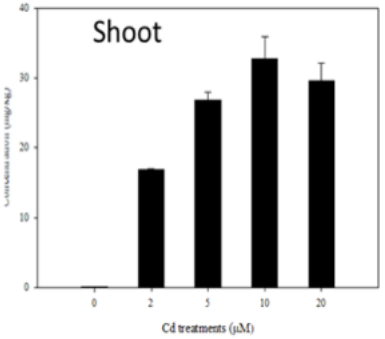

Bilecen et al., 2006
Yeşilırmak, F. et al . (2018)

Recombinant dMT is Intrinsically Disordered

dMT Purification

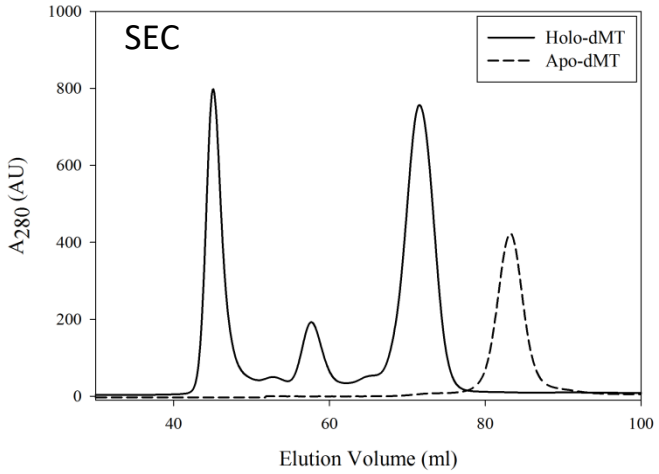

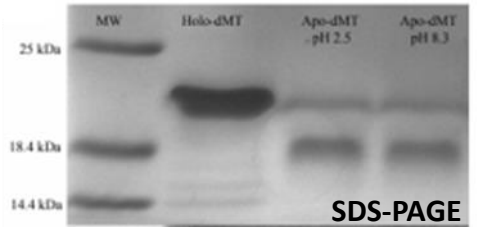

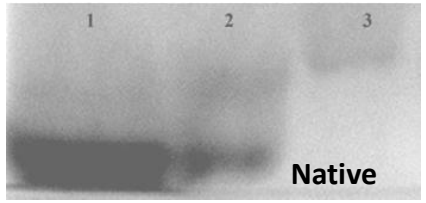

Holo-dMT: 10-16 kDa Apo-dMT: 8-9 kDa

Biophysical characterization of dMT

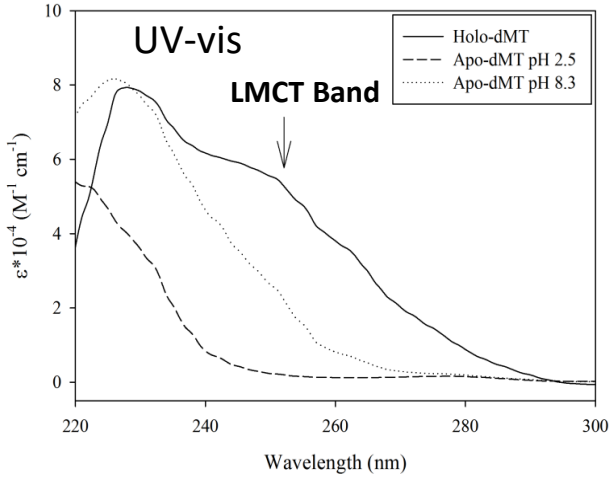

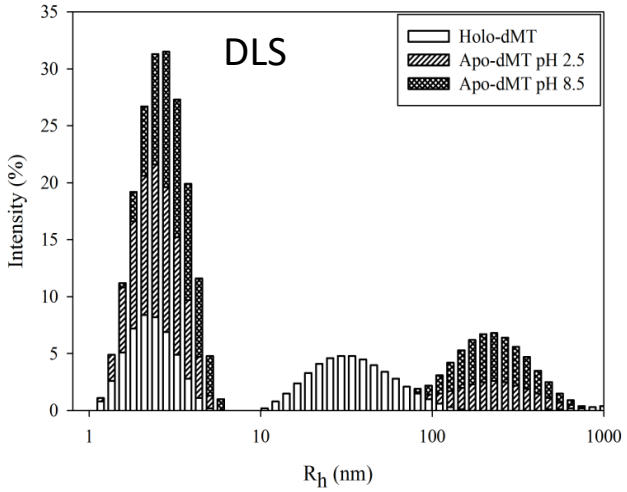

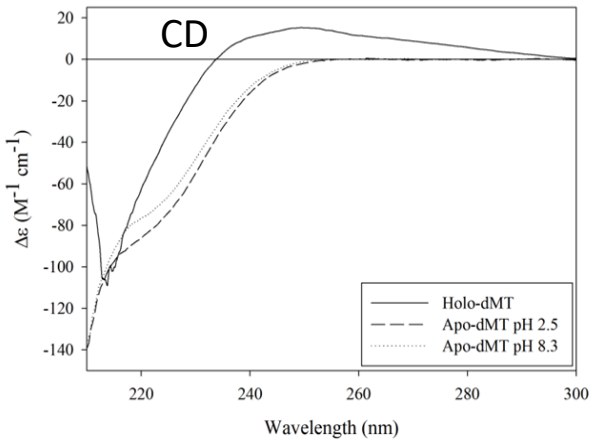

5.3±0.5 Cd ions/dMT
Cd-binding and structure are pH dependent.
dMT is an intrinsically disordered protein (IDP).

Yeşilırmak, F. (2008)
Aydın, M. (2011)

pH dependence of Cd binding and dMT folding

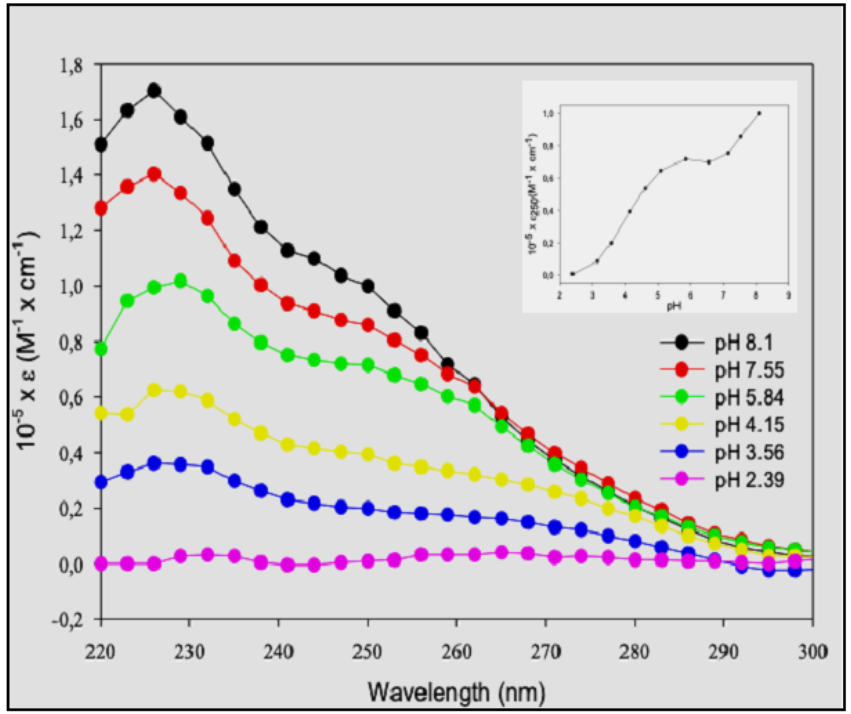

In UV-vis spectra ε_{250} values (inset) show two transitions at ~pH 7 and ~pH 5.

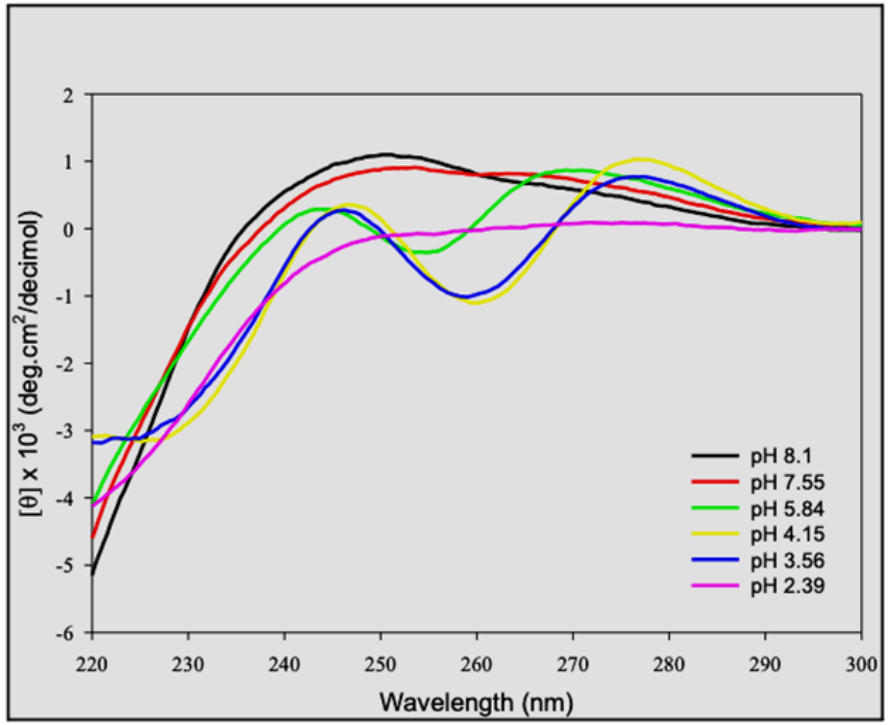

CD spectra show two maxima: 247 nm and 266 nm.
Loss of Cd diminishes the peak at 266 nm and 247 nm peak is shifted.

Different stabilities for the metal centers.

Solution Structure of dMT & Cd-binding

EOM: R_g Distributions &Models

Apo dMT

pH 2

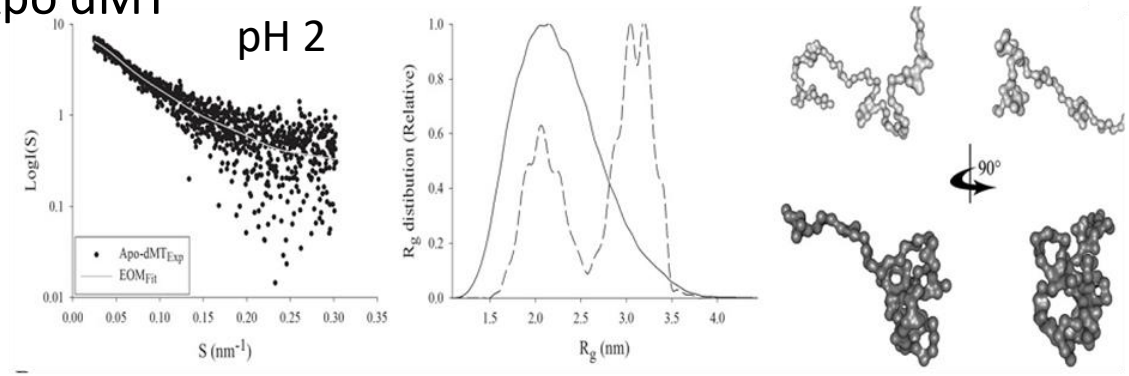

Holo dMT

PBS

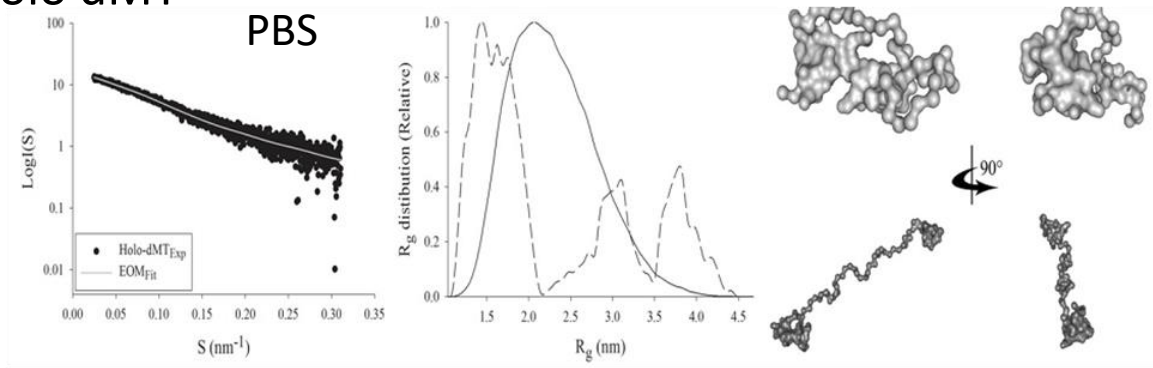

SAXS measurements on p12 beamline EMBL, Hamburg @Petra III, DESY.

ATSAS software for data analysis.

SAXS results show **co-existence of multiple conformations** in solution for both holo- and apo-dMT.

Flexibility of the apo dMT structure allows rapid binding of 5±1 Cd^{2+} leading to a more rigid structure.

Protein conformation and stability of metal centers are **pH dependent**.

In human body acidic conditions could result in the **release of the bound Cd^{2+}**.

Sayers et al. (2017)

Ferric binding protein (FbpA) from *Haemophilus influenzae*

H. Influenza is a gram-negative bacterium, causing upper respiratory tract infections. It is dependent on Fe for survival. When bacteria infect people, the necessary Fe is obtained from the host.

Fe hijacking mechanism

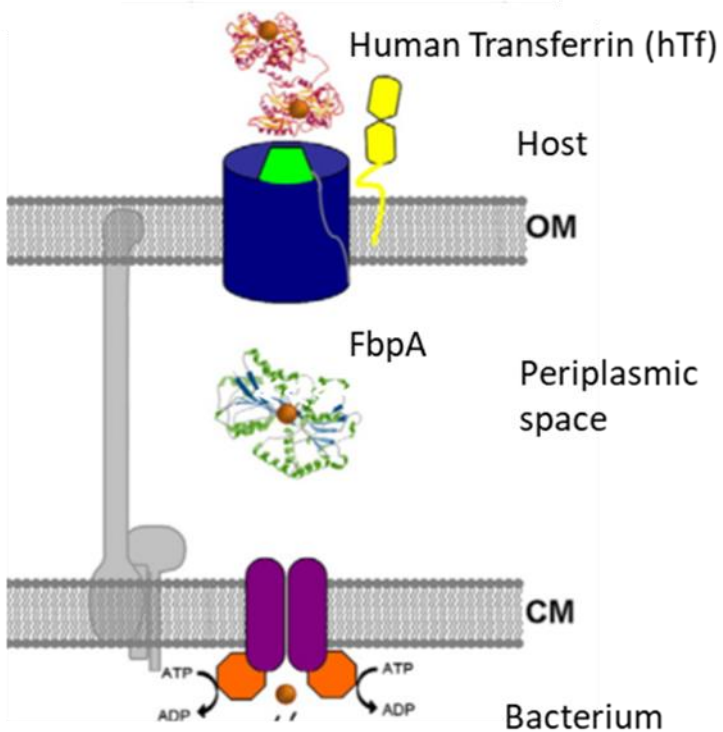

Siburt et al., et al. (2011))

Apo (1d9v; green) & holo-FbpA (1mrp; gray)

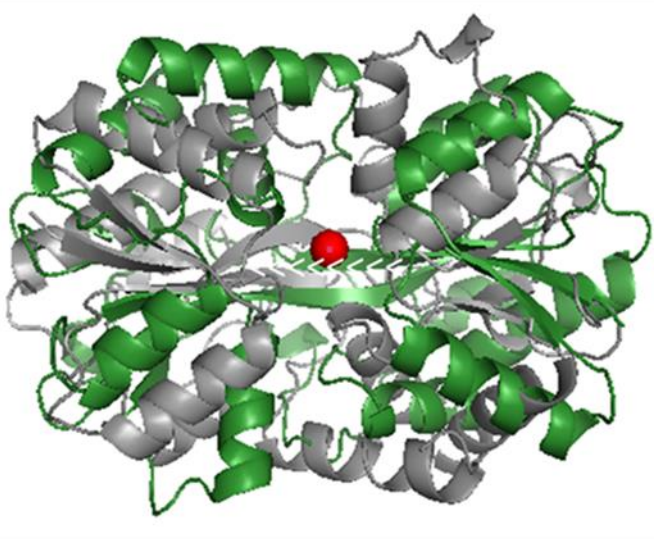

RMSD 0.26 nm

Question: What can the solution structures of holo- and apo-FbpA reveal about its Fe binding and release mechanisms? What is the effect of ionic conditions on Fe-binding?

Recombinant Wild type (WT) FbpA & D52A Mutant (PBS)

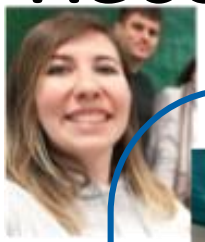

Ni-affinity :

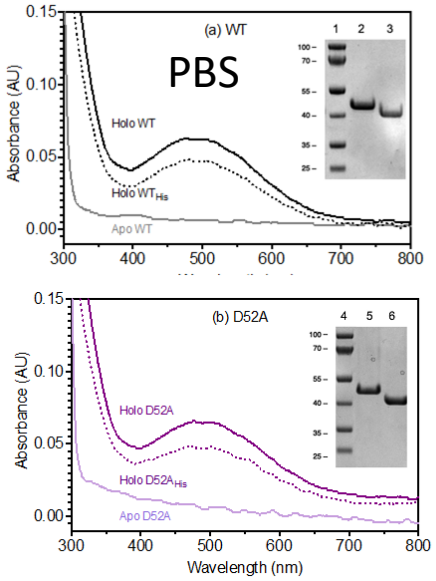

Purification: Proteins bind 0.8 Fe^{3+} /protein.
D52A migrates faster on SDS-PAGE analysis.
MD calculations: D52 is an allosteric site. D52A surface charge more positive.

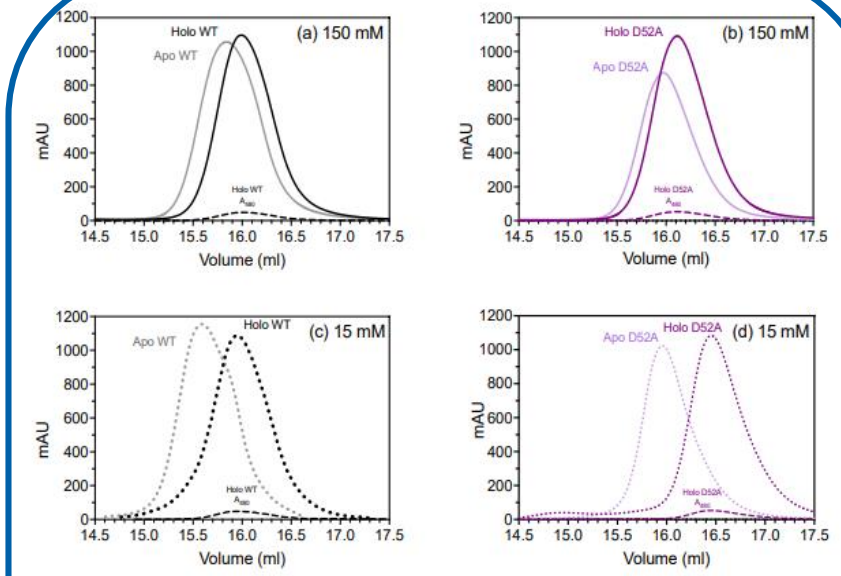

SEC results: apo proteins elute earlier than holo forms.
Smaller hydrodynamic radius for D52A.

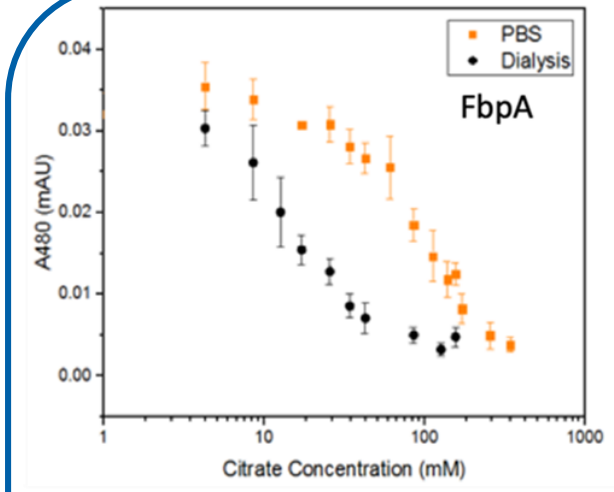

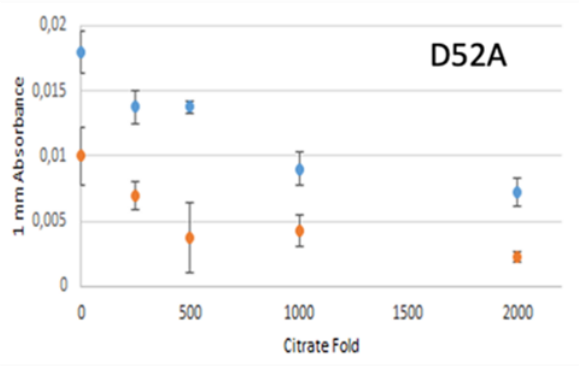

Fe-binding (citrate replacement assay): D52A releases Fe more readily than WT.

G. Liu et al, 2021, 2023

Conformational Differences Revealed by SAXS

Apo- and holo-FbpA both WT and D52A mutant were measured in low ionic strength (LIS) and high ionic strength (PBS) buffers.

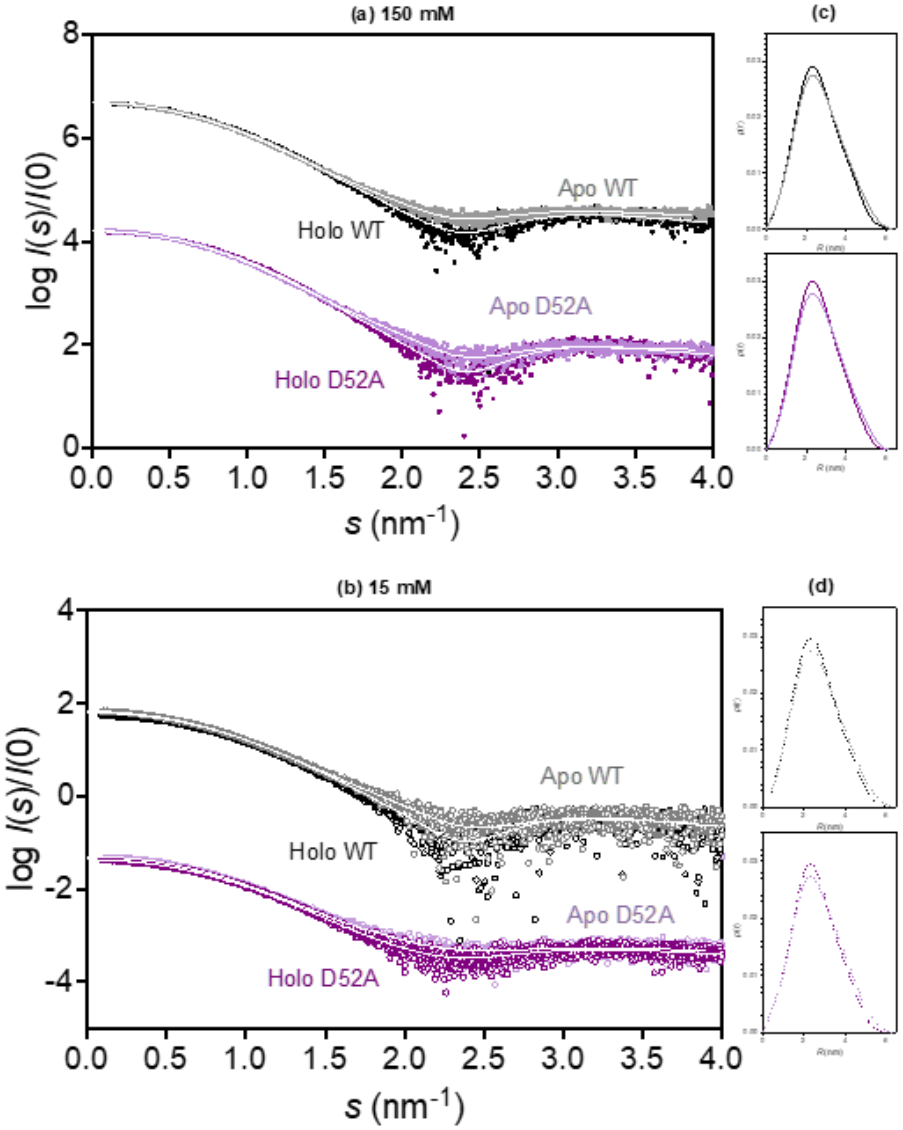

(a)

FbpA	150 mM		15 mM	
	Apo	Holo	Apo	Holo
χ^2	1.08	1.09	1.01	0.97
R_g (nm)	2.09±0.01	2.02±0.01	2.08±0.02	2.01±0.01
D_{max} (nm)	6.48±0.07	6.16±0.10	6.33±0.07	6.18±0.10
MM (Da)	29320	30060	29798	30596
Elution Volume (ml)	15.81	16.00	15.59	15.95

(b)

D52A	150 mM		15 mM	
	Apo	Holo	Apo	Holo
χ^2	1.03	1.16	1.10	1.00
R_g (nm)	2.05±0.01	1.98±0.01	2.07±0.01	1.97±0.01
D_{max} (nm)	6.16±0.10	5.93±0.10	6.46±0.24	5.92±0.24
MM (Da)	31618	29754	25996	26950
Elution Volume (ml)	15.97	16.11	15.96	16.45

Inline SEC-SAXS measurements on the p12 beamline EMBL, Hamburg @Petra III, DESY. ATSAS software for data analysis.

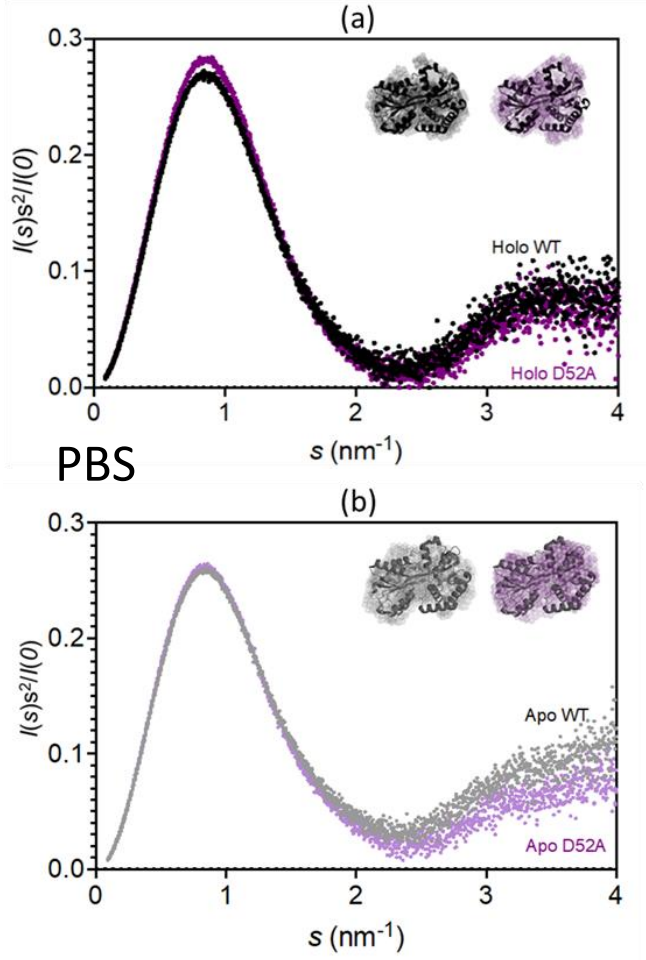

Apo forms are more extended than the holo forms.
A compaction of the structure is observed with D52A.

MD Simulations, SAXS Analyses & Crystal structures

1 ns apart snapshots from the MD simulations were collated together to form a pool of 1600 structures from the total of 1.6 µs trajectories.

System Label	Ionic Strength (mM)	RMSD(Å)
Apo WT	0	1.6 ± 0.3
Apo WT	150	1.8 ± 0.2
Apo D52A	0	1.0 ± 0.2
Apo D52A	150	1.4 ± 0.1
Holo WT	0	1.9 ± 0.2; 2.1 ± 0.2; 2.0 ± 0.2
Holo WT	150	1.4 ± 0.2; 1.8 ± 0.1; 1.8 ± 0.2
Holo D52A	0	1.2 ± 0.1; 1.4 ± 0.1; 1.4 ± 0.2
Holo D52A	150	1.7 ± 0.1; 1.2 ± 0.1; 1.3 ± 0.2

Average RMSD results from the 100 ns long MD simulations for WT and D52A mutant in apo (single run) and holo (three replicates) forms

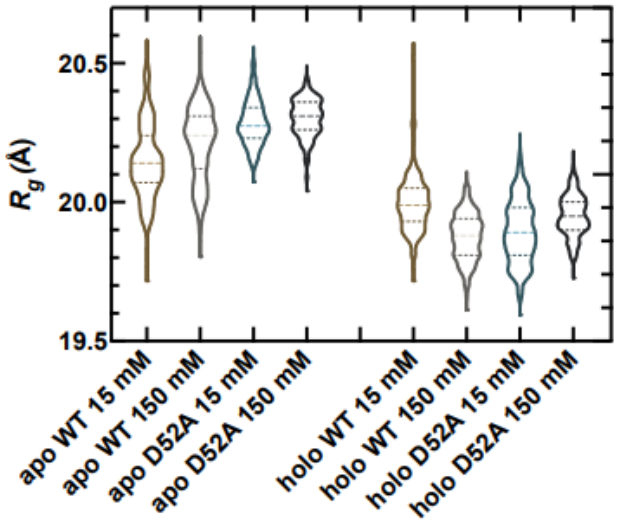

Violin plots of the Rg value distributions calculated from the simulations.
Dashed and dotted lines represent median and quartiles, respectively.

Protein	Ionic strength	Crystal structure fits		MD ensemble fits		
		χ^2	χ^2_{min}	Best Model	% single structures in pool with $\chi^2 \leq \chi^2_{min} + 0.05$	RMSD of best model from the respective X-ray structure (Å)
Apo WT	15 mM	1.03	1.03	Initial (X-ray) structure	22.4	0.
Apo WT	150 mM	1.25	1.15	Single snapshot from apo D52A 150 mM simulations	5.6	1.18
Apo D52A	15 mM	1.05	1.05	Initial (X-ray) structure	40.7	0.
Apo D52A	150 mM	1.09	1.02	Single snapshot from apo D52A 150 mM simulations	5.0	0.98
Holo WT	15 mM	1.00	1.00	Initial (X-ray) structure	0	0.
Holo WT	150 mM	1.36	1.00	Mixture of snapshots 78% Holo WT 150 mM (78%) / Apo WT 150 mM (22%) simulations	0 *	1.28 / 2.92
Holo D52A	15 mM	0.98	0.98	Initial (X-ray) structure	6.6	0.
Holo D52A	150 mM	1.18	0.99	Single snapshot from Holo WT 150 mM simulations	1.2	1.03

Goodness of fit of X-tal structures (1D9V/3OD7) to the SAXS data and best model fits to the ensemble generated by MD simulations. Results show that although crystal structures fit the LIS SAXS data agreement under native (PBS) conditions is poor.

Multiple Conformers of FbpA in PBS

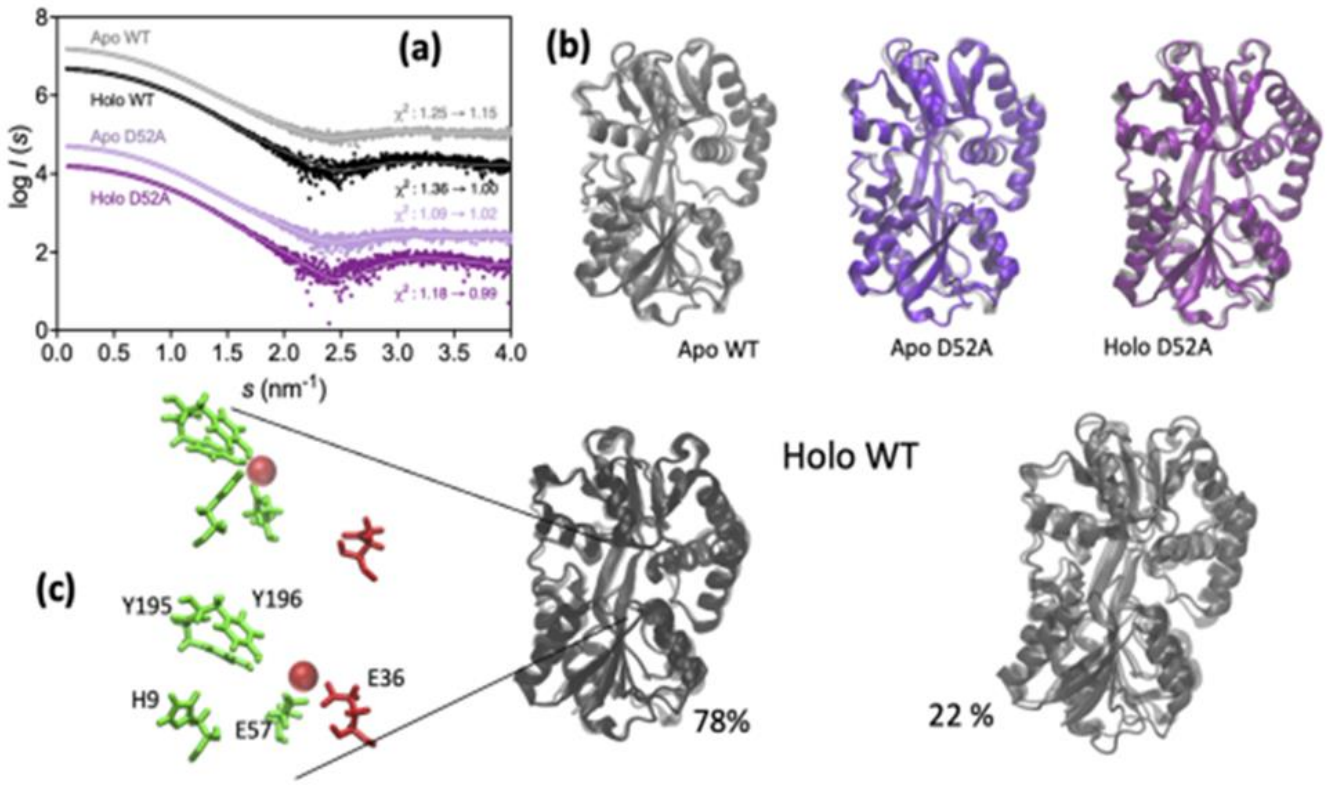

SAXS data allows detection of subtle conformational changes between apo- and holo-FbpA.

Structural flexibility of FbpA in **solution** in HIS (physiological) buffers can be detected by SAXS .

The multiple conformers co-existing in solution in HIS can be quantified by combining SAXS data with models generated by MD simulations

Results indicate that conformational selection model for ligand bind applies to FbpA and that changes in local conditions (ionic strength and pH) regulate metal binding.

Liu et al., 2023

Conclusions

Integration of information from biochemistry, molecular and structural biology and computational approaches are required to understand complex functional mechanisms in biological systems.

Synchrotron SAXS measurements are powerful structural characterization tools that can be pushed to their limits to provide data that can used in combination with MD simulations.

This combination allows to investigate dynamics of solution structures and complement the static crystal structure information.

We showed that for two structurally very different metal binding proteins structural flexibility results in co-existing multiple conformations in solution.

Structural flexibility responding to variations in local environments regulate mechanisms of metal binding and release in these proteins.

Acknowledgements

Sayers Group

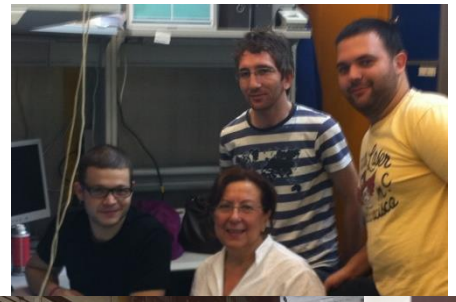

Thank you!

Sabanci University

Atılgan Group

bioSAXS group Group
EMBL-Hamburg

Financial Support: Turkish Atomic Energy Commission& TÜBİTAK